Dielectric Relaxations in Poly(di-*n*-alkyl itaconate)s

V. Arrighi and I. J. McEwen*

Chemistry Department, School of Engineering and Physical Sciences, Heriot-Watt University, Edinburgh EH14 4AS, United Kingdom

P. F. Holmes

DSM Research, PO Box 18, 6160 MD, Geleen, The Netherlands

Received March 5, 2004; Revised Manuscript Received April 22, 2004

ABSTRACT: The dielectric spectra for the series poly(dimethyl itaconate) to poly(di-*n*-octyl itaconate) have been measured and are discussed within the context of a main-chain−side-chain nanomorphology. The major dielectric event is associated with the calorimetric glass transition. In contrast to methacrylate family of polymers, it is not possible to detect separate contributions to this relaxation from a localized β-process and the cooperative backbone α-process. Different rotational barriers for each of the two side groups suggest that the β-process will be a broadened superposition of two relaxations. The longer side-chain itaconates show a second-high-frequency process which is assigned to the alkyl side chains relaxing independently within their own domains. This feature is absent in the corresponding methacrylates but is observed here to the greater level of nanophase formation in the itaconates and the presence of the second ester unit in the itaconate repeat unit structure. The longer side-chain di-*n*-alkyl itaconates exhibit two calorimetric glass transitions, and it is suggested that both the lower temperature glass transition and the high-frequency dielectric dispersion originate in the same side-chain relaxations.

Introduction

2-methylene butane-1,4-dioic acid, or itaconic acid, is structurally related to methacrylic acid by the replacement of one of the methyl hydrogen atoms by a second acid function.

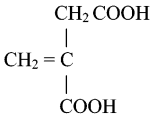

The polymerization of itaconic acid esters was first studied systematically around 50 years ago[1,2] and, in common with the methacrylates, the polymers are readily obtained via conventional free-radical methods,[3] although kinetic studies do show that some steric effects are present, especially with increasing side-chain size.[4−6]

Itaconic acid itself is actually a renewable resource obtained by fermentation from molasses[7] and much of the interest in the properties of itaconate polymers dates back to the 1970s, a decade which saw significant rises in the cost of hydrocarbon feedstocks. The difunctionality of the acid leads to degrees of structural variation absent from the methacrylate family, in that diesters, monoesters, and mixed esters[8] may all be polymerized, with polymers containing both cyclic anhydride and imide moieties also being accessible.[9−12] Polymers and copolymers based on the monoesters have been studied widely; these show interesting properties due to the free-acid function, such as interpolymer associates and blends,[13,14] hydrogel formation,[15] and polyelectrolyte and ionomeric behavior.[16,17] The diester-based systems, however, have attracted equal attention, since in many respects these should parallel the behavior and properties of the corresponding alkyl and aryl methacrylates.

* Corresponding author. E-mail: i.j.mcewen@hw.ac.uk; telephone: 0131 451 8030; fax: 0131 451 3180.

Although alike, these two polymer families are by no means identical, for example, viscometric data[18−20] indicate that itaconate polymer coils tend to adopt a rather extended chain conformation, with a preference for trans−trans diads.[21] Nonetheless, in the di-*n*-alkyl itaconate polymer series

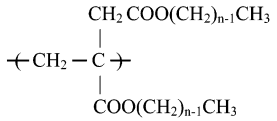

where *n* is the number of carbon atoms forming the ester chain, the glass-transition temperatures (T_g) are similar for the lower members of each series ($n < 6$), indicating a comparable chain flexibility. These T_g's also decrease with increasing side-chain length in a similar fashion, as would be expected from the internal plasticisation effect.[22] In the itaconates, however, a minimum in T_g versus *n* is obtained at $n \sim 6-7$, but then for the longer side chains ($n > 7$) the T_g values begin to increase again. At $n \sim 12$ and above, the side chains crystallize[23] and recent X-ray measurements[24] show that they do so in a paraffinic hexagonal lattice. Accompanying the increasing T_g values of the higher alkyl itaconates, at lower temperatures and additional to the T_g, dynamic mechanical spectra show the presence of a second major relaxation which has been ascribed to independent motion of the longer side chains.[25] This second relaxation correlates with a step change in the heat capacity[26,27] and so it has the necessary characteristic of a thermodynamic second-order transition, that is, it is a second glass transition, and this distinguishes it from the many other types of localized motions in glassy polymers which are not calorimetrically active. The same phenomenon can also be observed in copolymers[26] and in itaconate polymers with large and flexible cycloalkyl side units.[28]

10.1021/ma049553a CCC: $27.50
Published on Web 07/07/2004

Multiple glass transitions are, of course, a characteristic of phase-separated systems in which immiscible and usually structurally different moieties relax independently within their own domains. They were, at least initially, unexpected in the alkyl itaconates which would conventionally be regarded as typically amorphous structures. The model developed to account for the presence of two T_g's in the longer poly(di-*n*-alkyl itaconate)s was based, in part, on the agreement between the experimental heat capacity increment (ΔCp) at the lower temperature relaxation (T_g^L) and the value predicted by a partition function enumerating the heat capacity contributions arising solely from the conformational freedom of an *n*-alkyl chain.[27] At T_g^L, the side chains gain sufficient thermal energy to allow them to explore these numerous conformers and thus they can contribute detectably to the heat capacity. The main chain then relaxes independently at higher temperatures at the "normal" upper glass transition temperature (T_g^U).

The proposal that main chain and side chains could be regarded as independent units also evolved from examination of space-filling models.[29] The two ester links of the itaconate structure occupy much of the space in the immediate vicinity of the main chain and so effectively provide both a polar and steric barrier to any interaction with the alkyl side chains. The net result is that main chain and side chains are constrained to occupy different regions of space and, in a sense, they are separated into domains with differing conformational freedoms which thus relax independently. The differences in polarity are quite significant since, in itaconate polymers with oligo(ethylene oxide) side chains of comparable lengths, no evidence for a separate relaxation event is found.[29]

We have recently revisited the subject of domain structures in these otherwise amorphous polymers by analyzing X-ray data from a series of poly(di-*n*-alkyl itaconate)s.[30,31] The scattering patterns (an example is shown in Figure 11) show two peaks; one deriving from the nonbonded van der Waals distances and a second, well-defined peak whose position changes linearly with the number of CH_2 side-chain units. The dependence of this second spacing (d_{II}, interpreted by Miller et al. as the average correlation distance between adjacent main-chain segments[32]) was expressed as

$$d_{II} = d_O + n\, x_{CH2} \ldots \quad (1)$$

where $d_O = 8.15$ Å is an effective core diameter and $x_{CH2} = 1.27$ Å is the increase in d_{II}-spacing per CH_2 unit. The value d_O corresponds to a core size which includes both of the oxycarbonyl groups, so these data certainly support the notion of a nanoscale separation, or nanoheterogeneity, involving nonpolar alkyl side chains and the polar backbone. However, it is not possible to relate this form of domain structure directly with the appearance of the lower temperature relaxations (T_g^L) observed in the higher itaconates since nanoheterogeneity, in the form of a strong second d_{II} peak, is found irrespective of side-chain length, whether the polymer is above or below T_g^U and whether the polymer shows one or two T_g's.

The dynamic behavior of several poly(di-*n*-alkyl itaconate)s has also recently been reported by us, using quasielastic neutron scattering (QENS).[33] Here, significant relaxation processes can be detected well below the α-relaxation (the T_g) for all samples, but over temperature ranges which are dependent on the side-chain length. Interestingly, these obey time−temperature superposition, indicative of an underlying mechanism which is common to all the samples examined. In this present paper, we continue our investigations into the di-*n*-alkyl system and examine the dynamic behavior using dielectric spectroscopy. Diaz-Calleja et al. have previously reported the dielectric responses of several monoester, dicycloalkyl/diaryl, and lower dialkyl polymers,[34−39] but these workers concentrated their analysis on isochronal sub-T_g events associated with the side groups. In contrast to QENS, which returns information from all parts of a relaxing molecule, dielectric spectroscopy is of course primarily sensitive to modes involving dipolar units, and it is hoped by systematically examining the series poly(dimethyl itaconate) to poly(di-*n*-octyl itaconate) that this rather specific probe will provide further information on these intriguing polymers.

Table 1. Molar Masses and dsc Glass-Transition Values for the Poly(di-*n*-alkyl itaconate) Samples

	$10^4\, M_n$/g mol^{-1}	M_n/M_w	T_g/°C
poly(dimethyl itaconate)	5.9	1.23	100
poly(diethyl itaconate)	7.4	1.22	56
poly(di-*n*-propyl itaconate)	5.7	1.40	30
poly(di-*n*-butyl itaconate)	10.0	1.18	16
poly(di-*n*-pentyl itaconate)	12.0	1.48	6
poly(di-*n*-hexyl itaconate)	8.3	1.24	−19
poly(di-*n*-heptyl itaconate)	10.0	1.38	−23
poly(di-*n*-octyl itaconate)	19.0	1.40	−18

Experimental Section

Monomers and polymers were synthesized as described previously[18,19,22,23] and characterized by their NMR and infrared spectra. Polymer molar masses (Table 1), in terms of polystyrene equivalents, were measured on a Waters gpc system fitted with Polymer Laboratories mixed-C columns and using THF as solvent. Glass-transition temperatures were measured using a TA Instruments 2010 differential scanning calorimeter, fitted with a low-temperature facility, and scanning at 20 degrees per minute. These are reported in Table 1 as the midpoints of the inflections in the heat flow versus temperature trace.

Dielectric spectra were measured using a Solartron S1255 HF frequency response analyzer in conjunction with a S1296 dielectric interface over the frequency range $f = 1-10^6$ Hz. Polymers were placed between a pair of brass electrodes of 10-mm diameter; the lower electrode was fixed and the position of the upper adjustable by a micrometer. The electrode assembly was mounted in a thermostat linked to an Oxford Instruments ITC 503 temperature controller. Samples were heated to ~40 °C above their calorimetric T_g's and the electrode gap reduced to produce final specimen thicknesses in the region of 0.1−0.3 mm. Prior to measurements, samples were kept overnight at this temperature in a dry nitrogen atmosphere.

Conformational energy calculations were carried out using Allinger's molecular modeling program MM2.[40] The relative barriers to ester side group rotation were estimated using the heterotactic dimethyl itaconate trimer shown in Figure 1 since, in an atactic polymer, 50% of side-group environments will experience this environment. The two arrowed bonds (1 and 2 in the figure) attaching the two ester groups were rotated separately, minimizing the total energy at each step, and the potential energy profile versus rotation angle for each is shown in the two insets of Figure 1. The modeled rotations show discontinuities due to abrupt changes in molecular geometry but clearly indicate significantly different barrier maxima for complete rotation; for bond 1 it is ~50 kJ mol^{-1} whereas for bond 2 it is ~17 kJ mol^{-1}.

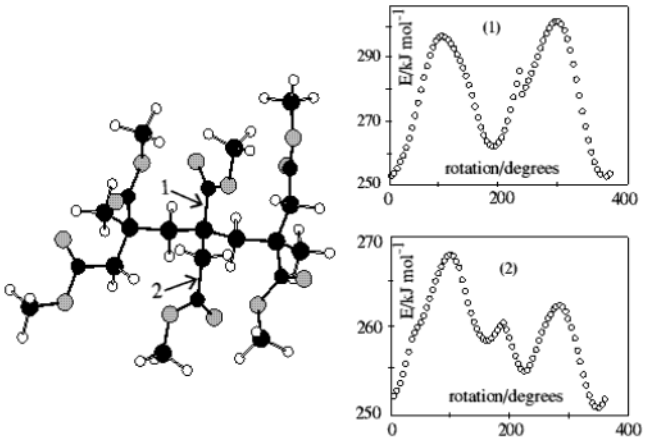

Figure 1. Dimethyl itaconate trimer, arrows indicate the rotated bonds. The upper inset shows the rotational energy profile for bond 1 and the lower inset shows the rotational energy profile for bond 2.

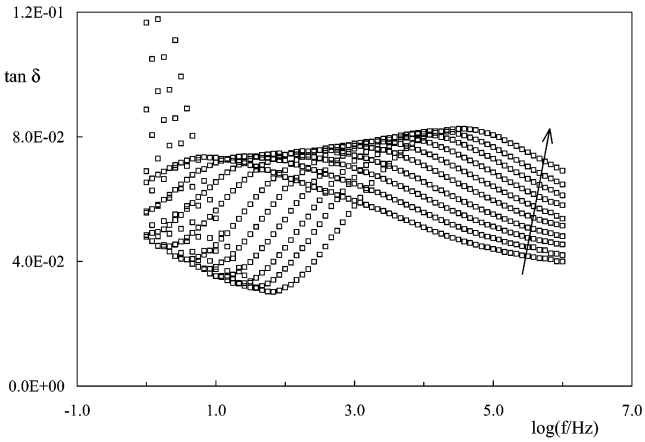

Figure 2. Dielectric relaxation (tan δ) for poly(dimethyl itaconate) from 107 to 145 °C at approximately four degree intervals in direction arrowed.

Results and Discussion

The Lower Itaconates. It is convenient to discuss the results for the shorter ($n \leq 4$) di-*n*-alkyl side-chain itaconate polymers together. Figure 2 shows the dielectric loss tangent for poly(dimethyl itaconate) in the temperature range above the calorimetric T_g, between 103 and 145 °C. The spectra show a broad relaxation peak which shifts to higher frequencies reflecting the decrease in relaxation time with temperature. At higher temperatures, there is a low-frequency conductivity contribution and also a slight narrowing of the relaxation peak. This behavior is rather similar to that shown by poly(methyl methacrylate)[41] which was interpreted by Williams et al.[42] in terms of the oxycarbonyl group motion where, as the temperature is increased, the increasing dynamic freedom of the main-chain backbone creates a more homogeneous environment for these relaxing dipoles and so leads to the observed peak narrowing. This picture can be readily recast in terms of the splitting or dynamic crossover region concept[43,44] in which the merging of two processes, the cooperative main chain or α-process (essentially the calorimetric T_g) and a localized β or Johari−Goldstein process,[45] occurs at a particular point in temperature-frequency space. These are observed as separate relaxations close to the T_g, but as a combined and narrowed "$\alpha\beta$" relaxation at higher temperatures.

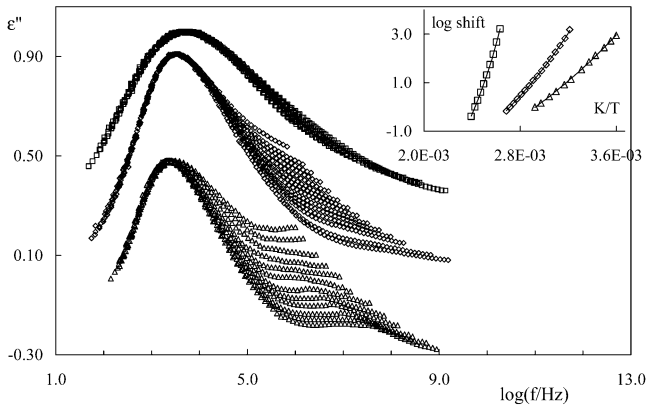

Figure 3. Shifted and normalized dielectric loss data for poly(dimethyl itaconate) (□); poly(di-*n*-butyl itaconate) (○); poly(di-*n*-octyl itaconate) (△). The shift factors are shown in the inset. Poly(di-*n*-octyl itaconate) data are displaced vertically for clarity.

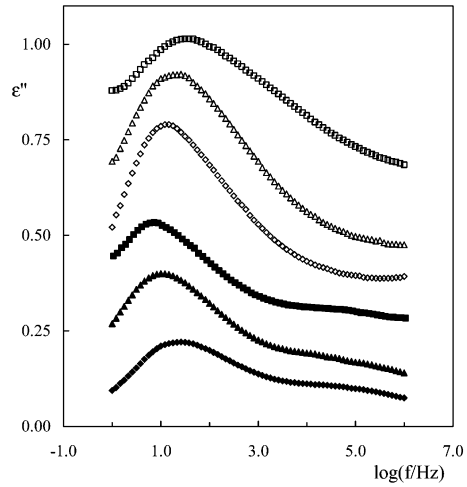

Figure 4. Loss curve for poly(dimethyl itaconate) (□) 115 °C; poly(diethyl itaconate) (△) 78 °C; poly(di-*n*-propyl itaconate) (◇) 70 °C; poly(di-*n*-pentyl itaconate) (■) 23 °C; poly(di-*n*-hexyl itaconate) (▲) 14 °C; poly(di-*n*-heptyl itaconate) (◆) 17 °C. Data are displaced vertically for clarity.

Figure 3 (upper data set) shows normalized and shifted dielectric loss curves for poly(dimethyl itaconate) where the inset illustrates that the temperature dependence of the relaxation maximum is non-Arrhenius. The poor superposition on the high-frequency flank reflects the temperature-narrowing effect, but it could also be taken as a visualization of two underlying process with different temperature dependences. Attempts at resolution by curve fitting (see below), however, proved rather unsatisfactory. The poly(dimethyl itaconate) data can be reasonably described using a single Havriliak−Negami function at each temperature, each with an unambiguous minimized set of parameters, but all attempts to improve the fits by adding a second function lead to ill-defined and unstable minima in parameter space, any one of which does not statistically improve the fit.

Figure 4 displays a representative set of isothermal dielectric loss spectra for the poly(di-*n*-alkyl itaconates) with $n = 1$, 2, 3, 5, and 6, which allow a general comparison within the series. Additionally, Figures 5 and 6 show the complete data sets obtained for poly(di-*n*-butyl itaconate) and poly(di-*n*-octyl itaconate). The overall trends with increasing length of side chain are evident from these figures: the width of the major

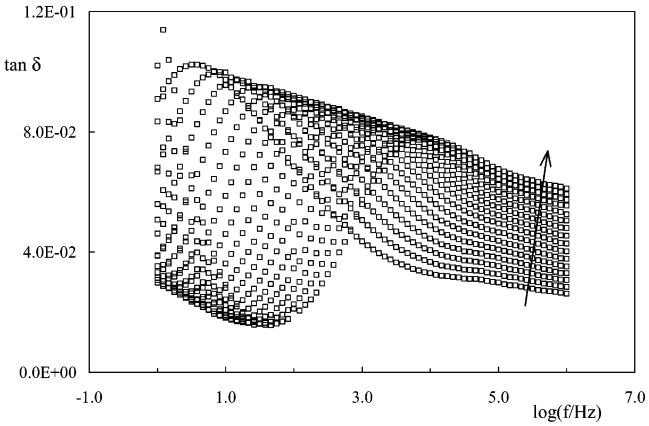

Figure 5. Dielectric relaxation (tan δ) for poly(di-*n*-butyl itaconate) from 38 to 116 °C at approximately four degree intervals in direction arrowed.

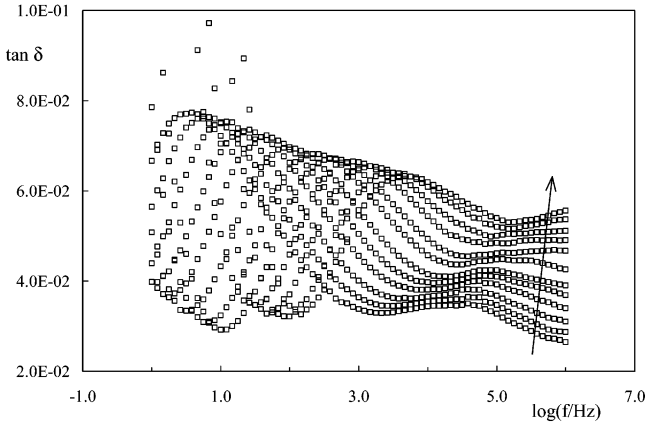

Figure 6. Dielectric relaxation (tan δ) for poly(di-*n*-octyl itaconate) from 5 to 69 °C at approximately five degree intervals in direction arrowed.

relaxation decreases, it occurs at lower temperatures within the frequency window, the relaxation strength decreases, and a low intensity event becomes more apparent. The shifted data for poly(di-*n*-butyl itaconate) and poly(di-*n*-octyl itaconate), also shown in Figure 3, illustrate this last point. Here, the normalized plots clearly show a side-chain-dependent process at the high-frequency end of the spectra with a different temperature shift dependence from the main relaxation.

Many studies of the relaxations associated with the glass transition have in recent years focused on the interelation of the cooperative main chain α-process with the localized Johari−Goldstein β-process.[43,44,46−48] At temperatures well above the T_g, these two molecular motions are combined into a single $\alpha\beta$ relaxation and, as the temperature is lowered, they "split" and map as two separate relaxations in an Arrhenius-type plot. The poly(*n*-alkyl methacrylates) have latterly proved a convenient test set for this since, by appropriate choice of side-chain length, the splitting region can be observed within an accessible temperature-frequency window for the chosen investigating technique. This approach has been adopted by Beiner and Donth's group using dielectric data from the lower alkyl methacrylate polymers.[44] They were able to resolve isothermal dielectric loss curves $\epsilon(\omega)$, obtained near T_g, into two components by curve-fitting their data to the sum of two Havriliak−Negami functions

$$\epsilon(\omega) = \sum_i \left[\frac{\Delta\epsilon_i}{(1 + (j\omega\tau_i)^{a_i})^{b_i}} + \epsilon_\infty \right] - j\left[\frac{\sigma}{\epsilon_v \omega^N} \right] \ldots \quad (2)$$

where a_i and b_i are the shape parameters, $\Delta\epsilon_i$ is the relaxation strength, ϵ_∞ is the dielectric constant at infinitely high frequency, $\omega = 2\pi f$ is the angular frequency, τ_i is the characteristic relaxation time, and $j^2 = -1$. The second term of eq 2 is included to account for conductive processes which are usually present at high temperatures; σ is the conductivity, ϵ_V is the vacuum permittivity, and the exponent $N \leq 1$.

These workers presented dielectric spectra for poly(ethyl methacrylate) and poly(*n*-butyl methacrylate) showing the development of a second relaxation, as a lower frequency shoulder, as the temperature is lowered toward T_g. The appearance of this second relaxation was identified with the splitting of the main-chain α-relaxation from the faster β-process, which itself becomes more localized as a specific side-group motion. Figure 7 is representative of a similar examination of the lower itaconates, where the data have been fitted to eq 2 by numerical minimization of the chi-square function[49] in the parameter space [σ, a_i, b_i, τ_i, $\Delta\epsilon_i$, $i = 1, 2$; $N = 1$]. In contrast to the methacrylate behavior, there are *no* discernible low-frequency shoulders (this is the case for all members of the itaconate series, see also figures 5−7) and, moreover, the minimization requires the second Havriliak−Negami function, labeled HN(2) in the figures, to be positioned as a high-frequency wing to obtain the statistical best fit. The upturn in the region of $f \sim 1$ Hz is due to conductivity entering the frequency window. Figure 7 shows also the deviations of the experimental data from the fitted function and although acceptably small these do not form a random pattern. Our conclusion is that a double Havriliak−Negami function is not the optimum choice of model for these data. One of course could add a further term, but since the data sets do not, at least visually, comprise three relaxations we choose not to do so. In this respect, we also should point out that the Havriliak−Negami (2) curves shown in Figure 7 for both poly(di-*n*-propyl itaconate and poly(di-*n*-butyl itaconate) cannot be positioned unambiguously on the frequency axis. These are especially insensitive to the τ_2 value and several distinct parameter sets $\{a_2, b_2, \tau_2, \Delta\epsilon_2\}$ lead to equally acceptable fits.

It seems then that an $\alpha\beta$ splitting event is not observable or not resolvable in the lower itaconates, at least not within the frequency−temperature ranges examined here. There is no obvious reason both a faster side chain and a slower main chain relaxation should not be present, and indeed a β-process is observed in the isochronal mechanical spectra[22] of these polymers, just as it is in the methacrylates.[41] A possible reason for our observations can be offered. First, the two side group dipoles are attached differently to the main chain and so their rotational barriers will also be different. The results of our MM2 calculations on the model trimer are shown in Figure 1 and certainly bear this out; the maximum barrier for the methylene−ester complete rotation (bond 2) is just one-third that of the corresponding main chain−ester rotation (bond 1). Each dipole consequently will relax with different relaxation times, and the distribution of local environments will also be different, leading to two different distributions of relaxation times. This will produce a wider overall

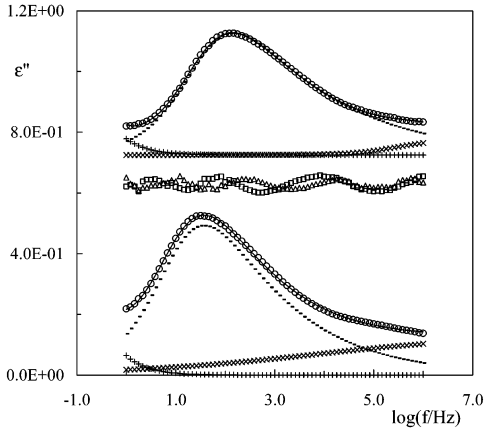

Figure 7. Experimental data (○) for poly(di-*n*-propyl itaconate) at 86 °C (upper curve, shifted for clarity) and poly(di-*n*-butyl itaconate) at 54 °C (lower curve). Full lines are the best fits of eq 2: (+) conductivity; (—) HN(1); (×) HN(2). Deviation patterns: (△) poly(di-*n*-propyl itaconate); (□) poly(di-*n*-butyl itaconate) are shown at 5× magnification.

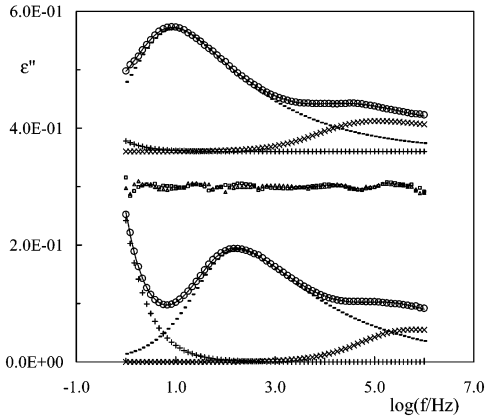

Figure 8. Experimental data (○) for poly(di-*n*-octyl itaconate) at 13 °C (upper curve, shifted for clarity) and at 36 °C (lower curve). Full lines are the best fits of eq 2: (+) conductivity; (—) HN(1); (×) HN(2). Deviation patterns: (△) 13 °C; (□) 37 °C are shown at 5× magnification.

spectrum of relaxation times for dipolar realignment than operates in the methacrylates, and consequently a broader and less easily resolvable dielectric dispersion will result. Our calculations, of course, neglect matrix effects and so the above must be regarded as a first-order approach to the problem, giving an idea only of the *relative* magnitude of these two barriers.

Another structural effect could hinder resolution of the underlying α and β components and this relates to main-chain−side-group coupling. The nonpolar main-chain motion is dielectrically active by virtue of the attached oxycarbonyl dipole[41,50] and such a coupling is evident even below T_g in methacrylate polymers.[51,52] If this dipole is progressively decoupling by intervening chemical bonds the weaker will become the dielectric signature from main-chain motion, most especially near the onset of the $\alpha\beta$ splitting region. The second ester unit in the itaconates will be partially decoupled by its methylene linkage and so be less responsive to main-chain motion compared with the directly attached dipole, thus producing a further broadening effect that will hinder experimental observation of these two contributions.

The Higher Itaconates. We turn now to the higher itaconates, whose dielectric spectra show more clearly

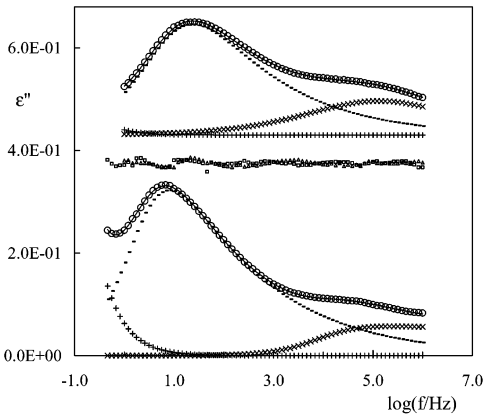

Figure 9. Experimental data (○) for poly(di-*n*-heptyl itaconate) at 17 °C (upper curve, shifted for clarity) and poly(di-*n*-pentyl itaconate) at 23 °C (lower curve). Full lines are the best fits of eq 2: (+) conductivity; (—) HN(1); (×) HN(2). Deviation patterns: (△) poly(di-*n*-heptyl itaconate); (□) poly(di-*n*-pentyl itaconate) are shown at 5× magnification.

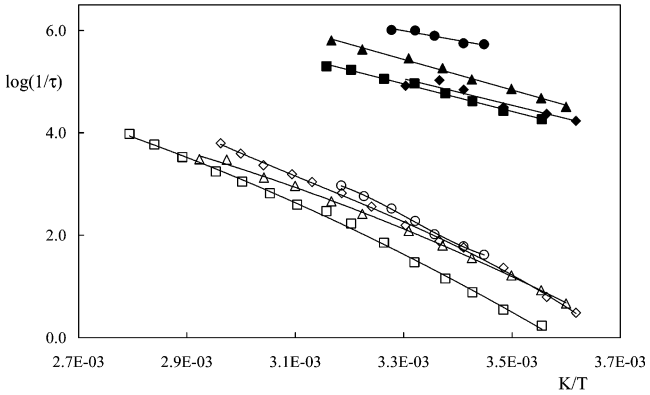

Figure 10. Havriliak−Negami parameters τ_1 (open symbols) and τ_2 (filled symbols) for poly(di-*n*-pentyl itaconate) (□ ■); poly(di-*n*-hexyl itaconate) (◇ ◆); poly(di-*n*-heptyl itaconate) (○ ●); poly(di-*n*-octyl itaconate) (△ ▲).

the second dispersion that appears as high-frequency broadening in the lower members (compare Figures 2−6). Figure 8 shows the fits to the poly(di-*n*-octyl itaconate) data at two representative temperatures obtained using eq 2. The data here are well-described by the sum of two Havriliak−Negami terms, with smaller and more random deviations than those displayed in Figure 7. It would appear that two distinct relaxation processes can now be resolved in this polymer. A similar picture is presented in Figure 9 which shows representative fitted curves for poly(di-*n*-pentyl itaconate) and poly(di-*n*-heptyl itaconate). These dielectric data show that the di-*n*-alkyl itaconate polymers have a second, weaker, high-frequency (low-temperature) relaxation which resolves within the frequency window as the side-chain length increases. Figure 10 plots the Havriliak−Negami relaxation times obtained for the higher itaconates, showing the main relaxation (τ_1) to be non-Arrhenius in each case. The values for τ_2 in Figure 10 are restricted to the lower temperatures runs of each sample, where a reasonable expression of the second relaxation contour is available, giving an acceptable confidence in the fitted parameters. Treating the temperature dependences of $\log(1/\tau_2)$ as Arrhenius, the apparent activation energies (E_{app}) for this process may be estimated and these are summarized in Table 2.

Table 2. Activation Energies (E_{app}) for the Second Relaxation, T_g at 0.1 Hz and the Fragility Index (m)

	m	T_g/°C (0.1 Hz)	E_{app}/kJ mol^{-1}
poly(dimethyl itaconate)	61	97	
poly(diethyl itaconate)	40	57	
poly(di-*n*-propyl itaconate)	27	43	
poly(di-*n*-butyl itaconate)	27	23	
poly(di-*n*-pentyl itaconate)	25	−2	52
poly(di-*n*-hexyl itaconate)	26	−10	49
poly(di-*n*-heptyl itaconate)			∼40
poly(di-*n*-octyl itaconate)	20	−14	55

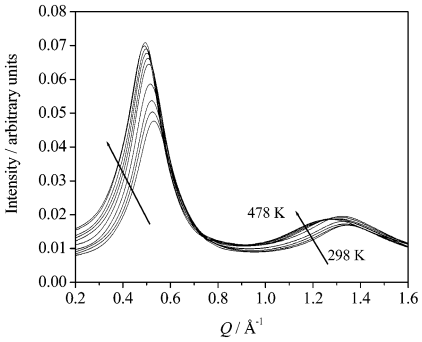

Figure 11. X-ray patterns for poly(di-*n*-propyl itaconate) at temperatures between 298 and 478 K. Q is the scattering vector. Data taken from ref 59.

Wada et al.[53] reported weak dielectric relaxations at ∼120 K in several polymethacrylates which they ascribed to specific rotations of the alkyl side chains. However, these occur in a different region of temperature−frequency space from the high-frequency itaconate relaxation, whose molecular origin must lie elsewhere. As far as we are aware, dielectric studies have not been able to detect an equivalent relaxation in the methacrylates, although the presence of a low-temperature "glass transition" in the higher methacrylates is proposed by Beiner and Donth's group on the basis of rheometric data and a loss event detected by temperature-modulated dynamic calorimetry.[46,54,55] These authors also discuss X-ray scattering patterns from which they infer a nanodomain structure for the methacrylates similar to, but somewhat less well-developed than, that found for the itaconates[30,31] (see below, Figure 11). They label the low-temperature transition α_{PE} to emphasize its polyethylene-like nature, that it is restricted to the alkyl side chain nanodomains, and it is dielectrically inactive. On the other hand, the dielectric spectra presented by Floudas et al. for poly(*n*-lauryl methacrylate) and poly(*n*-decyl methacrylate)[56,57] do provide evidence of a weak high-frequency relaxation which they call a "fast β" process. This particular relaxation maps in a very similar position to our τ_2 data shown in Figure 10 and is assigned by them to hindered rotational movements of the side chains. The activation energy for the fast β process is 48 kJ mol^{-1}, comparable to those in Table 2 and close to that found mechanically for polyethylene.[58]

By analogy with the methacrylate behavior discussed above, but more pertinently from the observed correlation and development of the itaconate high-frequency relaxation with side-chain length, we suggest the molecular origin of this relaxation is indeed side-chain motion and, further, that it is likely to be the dielectric analogue of the T_g^L discussed in the Introduction. However, relative to the methacrylate α_{PE} or fast β processes, the two obvious differences are (a) it is calorimetrically active in the thermodynamic sense and (b) it is dielectrically observable as a separate relaxation

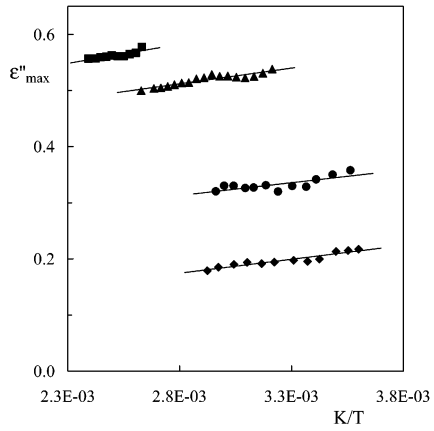

Figure 12. Dielectric loss maxima for poly(dimethyl itaconate) (■); poly(di-*n*-butyl itaconate) (▲); poly(di-*n*-hexyl itaconate) (●); poly(di-*n*-octyl itaconate) (◆).

peak of modest strength. The calorimetric manifestation of α_{PE} in the methacrylates is limited to the imaginary component of the so-called complex heat capacity, obtained from temperature-modulated scanning calorimetry,[55] rather than a "classic" glass transition as in the itaconates. We suggest this is a consequence of a better-developed nanostructure in the itaconates, as can be seen by comparing Figure 11 with the X-ray data presented in refs 54 and 56 for the corresponding poly(*n*-propyl methacrylate). The d_{II} peak at $Q \sim 0.5$ Å^{-1} is a full order of magnitude larger in the itaconate, and so there are many more scattering elements separated by this characteristic distance in this polymer. Consequently, a greater volume fraction of itaconate side chains are involved in nanodomains and therefore respond in a manner akin to that of conventional two-phase systems which more clearly display the relaxation behavior of each phase.

Turning to the dielectric activity of the itaconate alkyl side chains, this must result from coupling of the side-chain movement to the oxycarbonyl dipole. Apart from the weak contributions to the dielectric spectra of the two higher methacrylate homologues noted above,[56,57] the side-chain motions of methacrylates are dielectrically inactive and so must be virtually uncoupled from this dipole or, equivalently, the dipole is sufficiently immobilized by its local environment.[60] The dielectric activity observable in the itaconates most likely occurs because of the structural difference between the two side chains. While one of the ester links is "methacrylate-like", in that it is directly attached to the main chain and must encounter a similar local environment, the other is relieved of some restrictions by virtue of the intervening methylene group as noted earlier. It should consequently be able to move more readily, and at lower temperature, in response to alkyl side chain movements.

Further contrasts between itaconate and methacrylate dielectric behavior can be noted. Data for the methacrylates[41,42,44,45] show that the α-relaxation intensity increases with increasing temperature, which is the converse of the $1/T$ proportionality classically expected for noninteracting dipoles,[41] and so indicates that the redirection of the relaxing dipole is hindered by the local environment at low temperature. The temperature dependence of the relaxation intensity for the itaconates is exemplified in Figure 12, where a $1/T$ dependence is indeed seen to operate. This points to weaker dipole−environment interactions, even in the

region of decreasing free volume close to T_g, and this extra freedom is probably associated with the more mobile methylene-linked second ester group.

When discussing poly(*n*-decyl methacrylate), Floudas and Stepanek[56] proposed that concentration fluctuations caused a broadening of the α-relaxation in that polymer. The idea is that the backbone encountered a variety of local environments because of a heterogeneous side-chain environment. Despite the presence of two (different) dipoles per main-chain unit, the dispersions of the higher itaconates are not especially broad. This could indeed also be due to heterogeneity effects or more particularly to a lack of heterogeneity. At the molecular level, the itaconate unit is almost symmetric in size and shape compared to the methacrylate unit, and so this intrinsic element of heterogeneity is absent. Also, we have already remarked on the degree of nanostructural organization in the itaconates and that a large fraction of side chains are located within alkyl domains so, as a whole, the alkyl chain environment itself should be less heterogeneous.

Fragility of Itaconate Polymers. The relaxation times for covalent network glasses show Arrhenius behavior in the temperature range above their glass transitions. Departure from Arrhenius behavior is common for polymeric glasses and is referred to as "fragile" behavior, whereas glasses following Arrhenius behavior are said to be "strong". If relaxation times $\tau(T)$ are plotted as log τ against T_g/T, the slope at the glass transition defines the dynamic fragility

$$m = \frac{d(\log \tau)}{d(T_g/T)} \tag{3}$$

where m is an index of how rapidly the relaxation time (or viscosity) increases on approaching structural arrest at the glass transition.[61] Fragile polymers have a higher slope and their relaxation time changes considerably through the glass temperature, while strong polymers show much less property change in the transition region. Structural characteristics which restrict segmental motion will render polymers more fragile. For strong systems, a lower limit of fragility of $m \sim 16$ has been established, whereas more fragile systems tend to have $m \sim 100$ or more.[62]

It is useful to compare the temperature dependences of the relaxations for the itaconate series using this approach, as is shown in Figure 13, where the characteristic relaxation time has been taken as the inverse frequency of the dielectric peak maximum. T_g is operationally defined as corresponding to a relaxation time of 10 s and is located by short extrapolation after fitting the data to the Vogel−Tamman−Fulcher equation. Table 2 shows these 0.1 Hz T_g values, which closely follow the calorimetric transitions in Table 1, and also the values of m for the series. Poly(dimethyl itaconate) is thus a fragile polymer but the variation in m indicates a change from a fragile to a strong liquid with increasing length of side chain. This change is nonlinear in both n and the nanostructure parameter d_{II} (through eq 2). The greatest decrease occurs with the chain extension of the first two methylene units, thereafter the fragility appears to close on a limiting value. Analogous trends are reported for the methacrylates[56,57] and for the α-*n*-alkyl methacrylates.[63]

The fragility index m is correlated with the KWW function exponent β_{KWW};[62] higher values of fragility correspond to lower β_{KWW} values which also indicate a broader relaxation spectrum. Figure 13 can also be regarded as a cooperativity plot through the coupling parameter $n^* = 1 - \beta_{KWW}$,[64] and so it shows that the relaxation of poly(dimethyl itaconate) is highly cooperative but that the dynamic constraints are appreciably diminished with increasing length of side chain. The explanation for this progressive change in fragility must surely be associated with the CH_2 structural increment; however, one should proceed cautiously since we are dealing here with a nanoheterogeneous system and not the type of fluid from which the concepts of fragility and cooperativity were developed. That being said, an attractive explanation of the effect is one which actually appeals to the heterogeneity of the system. The alkyl nanodomains are fully mobile at temperatures below, or frequencies above, the α-relaxation and, on the basis of the fragility data for polyethylene, such alkyl chain mobility will be a low cooperativity process.[57] So, as the itaconate side chain lengthens, the requirement for main-chain cooperativity diminishes as the number of backbone−backbone contacts decrease (as d_{II} in eq 1 increases) and are replaced by the weaker restraining effects of the alkyl domains. The main α-relaxation thus evolves as an increasingly less fragile event on moving up the poly(di-*n*-alkyl itaconate) series. It is also evident that an alkyl nanodomain size corresponding to 3- or 4-carbon side chains efficiently suppresses backbone cooperativity (Figure 13, inset) and that increasing the domain size further has little effect.

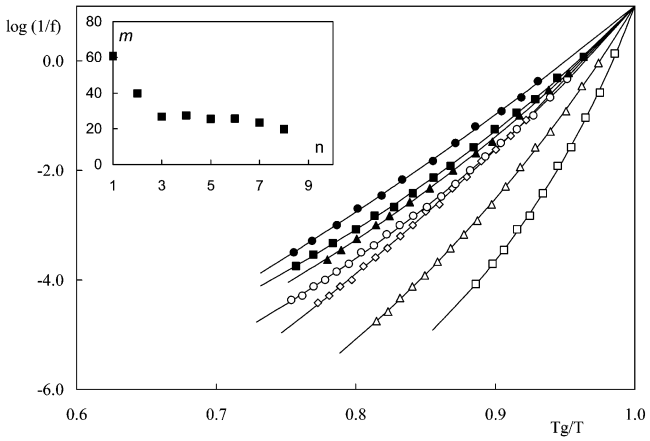

Figure 13. Fragility plots for poly(di-*n*-alkyl itaconate)s: $n = 1$ (□); $n = 2$ (△); $n = 3$ (◇); $n = 4$ (○); $n = 5$ (■); $n = 6$ (▲); $n = 8$ (○). Full lines are fits to the VTF equation. Inset shows the fragility index (m) vs number of side-chain carbons.

Conclusions

We have obtained the dielectric spectra for a series of di-*n*-alkyl itaconate polymers, ranging from the dimethyl to the dioctyl esters. The data have been discussed within the context of a nanomorphology in which the main chain and the side chain occupy separate domains. The major dielectric event involves the ester dipoles responding to the relaxations which are associated with the calorimetric glass transition. This dielectric peak moves to lower temperatures and higher frequencies with increasing side-chain length, reflecting the plasticising effect of the alkyl units, in a manner similar to the poly(*n*-alkyl methacrylates). However, in contrast to methacrylate polymers, it is not possible to detect separate contributions to the main relaxation from a localized Johari−Goldstein β-process

and a cooperative backbone α-process. On the basis of estimated relative rotational barriers for each of the two ester side groups, it is suggested that the β-process in the itaconates will be a broadened superposition of relaxations from each of these, and so their contributions will be difficult to resolve.

The high-frequency side of the main itaconate dielectric dispersion progressively changes in shape as the side-chain length increases, and superposition indicates that a secondary high-frequency (low-temperature) process is the cause. This second process can be resolved by curve fitting the data to two Havriliak−Negami functions for chain lengths greater than five carbons and can be clearly seen as a separate, if weak, relaxation for poly(di-*n*-octyl itaconate) within the temperature−frequency window used. This second itaconate dispersion is assigned to the alkyl side chains relaxing independently of the main chain within their own domains. The corresponding feature is absent from the dielectric spectra of the methacrylates, but the ability to observe this event in the itaconates may be associated with a greater number of alkyl units incorporated into discrete nanodomains and to the significant structural difference between the itaconates and methacrylates, namely, the second, relatively mobile, ester unit in the itaconate structure which is uncoupled from the main chain by a CH_2 unit.

The longer di-*n*-alkyl itaconates exhibit two calorimetric glass transitions and it is inferred that both the lower temperature glass transition T_g^L and the high-frequency dielectric dispersion originate in the same relaxation. It is calorimetrically unobservable below a side chain length of ∼6 (calorimetric activity is related to the number of available conformers and so T_g^L is apparent only above this chain length) whereas the dielectric equivalent is found at all chain lengths. If, as is being argued, the high-frequency itaconate relaxation is a T_g-like (cooperative) molecular event, it should exhibit a typically curved trace in an Arrhenius plot. The τ_2 data in Figure 10 are too limited to draw conclusions in this regard, although those for poly(di-*n*-pentyl itaconate) and poly(di-*n*-octyl itaconate) are indeed statistically better described by curves on the basis of smaller correlation coefficients. Future investigations of these polymers are indicated and should prove interesting. A preliminary publication[65] on the direct observation of molecular motion in poly(di-*n*-octyl itaconate) by NMR has been published recently which provides direct evidence that the T_g^L relaxation can be attributed to motions of the whole alkyl side chain. Further work, especially modeling studies and solid-state nmr, is needed to give a fuller understanding of the dynamics of the second ester function and its alkyl chain.

References and Notes

(1) Knuth, C. J.; Bruins, P. F. *Ind. Eng. Chem.* **1955**, *47*, 572.
(2) Marvel, C. S.; Shepherd, T. H. *J. Org. Chem.* **1959**, *24*, 599.
(3) Tate, B. E. *Adv. Polym. Sci.* **1967**, *5*, 214.
(4) Sato, T.; Takahashi, Y.; Seno, M.; Nakamura, H.; Tanaka, H.; Ota, T. *Makromol. Chem., Chem. Phys.* **1991**, *192*, 2909.
(5) Tomic, S. L.; Filipovic, J. M.; Velickovic, J.; Katsikas, L.; Popovic, I. G. *Macromol. Chem. Phys.* **1999**, *200*, 2421.
(6) Yee, L. H.; Coote, M. L.; Chaplin, R. P.; Davis, T. P. *J. Polym. Sci., A: Polym. Chem.* **2000**, *38*, 2192.
(7) Kane, J. H.; Finlay, A. C.; Amann, P. F. U.S. Patent 2,385,-283, 1945.
(8) Cowie, J. M. G.; Yasdani-Pedram, M.; Ferguson, R. *Eur. Polym. J.* **1985**, *21*, 227.
(9) Cowie, J. M. G.; Reid, V. M. C.; McEwen, I. J. *Br. Polym. J.* **1990**, *23*, 352.
(10) Sato, T.; Takarada, A.; Tanaka, H.; Ota, T. *Makromol. Chem., Macromol. Chem. Phys.* **1991**, *192*, 2231.
(11) Bell, S. Y.; Cowie, J. M. G.; McEwen, I. J. *Polymer* **1994**, *35*, 786.
(12) Otsu, T.; Yang, J. Z. *Polym. Int.* **1991**, *25*, 245.
(13) Velada, J. L.; Cesteros, L. C.; Katime, I. *Macromol. Chem. Phys.* **1996**, *197*, 2247.
(14) Katime, I.; Meaurio, E.; Cesteros, L. C.; Mendiziba, l E. *Appl. Spectrosc.* **2003**, *57*, 829.
(15) Barcellos, I. O.; Pires, A. T. N.; Katime, I. *Polym. Int.* **2000**, *49*, 825.
(16) Gargallo, L.; Radic, D.; Yasdani-Pedram, M.; Horta, A. *Eur. Polym. J.* **1989**, *25*, 1059.
(17) Song, J. M.; Kim, S. H.; Kim, J. S. *Abstr. Pap. Am. Chem. Soc. 99-Poly(2)* **2002**, 223.
(18) Velickovic, J.; Filipovic, J.; Coseva, S. *Eur. Polym. J.* **1979**, *15*, 521.
(19) Velickovic, J.; Filipovic, J. *J. Makromol. Chem.* **1984**, *185*, 569.
(20) Yasdani-Pedram, M.; Gargallo, L.; Radic, D. *Eur. Polym. J.* **1985**, *21*, 461.
(21) Saiz, E.; Horta, A.; Gargallo, L.; Hernandez-Fuentes, I.; Racic, D. *Macromolecules* **1988**, *21*, 1736.
(22) Cowie, J. M. G.; Henshall, S. A. E.; McEwen, I. J.; Velickovic, J. *Polymer* **1977**, *18*, 612.
(23) Cowie, J. M. G.; Haq, Z.; McEwen, I. J.; Velickovic, J. *Polymer* **1981**, *22*, 327.
(24) Lopez-Carrasquero, F.; de Ilarduya, A. M.; Cardenas, M.; Carrillo, M.; Arnal, M. L.; Laredo, E.; Torres, C.; Mendez, B.; Muller, A. J. *Polymer* **2003**, *44*, 4969.
(25) Cowie, J. M. G.; Haq, Z.; McEwen, I. J. *J. Polym. Sci., Polym. Lett. Ed.* **1979**, *17*, 771.
(26) Cowie, J. M. G.; McEwen, I. J.; Yasdani-Pedram, M. *Macromolecules* **1983**, *16*, 1151.
(27) Cowie, J. M. G.; Ferguson, R.; McEwen, I. J.; Yasdani-Pedram, M. *Macromolecules* **1983**, *16*, 1155.
(28) Cowie, J. M. G.; Ferguson, R.; Mathieson, K.; McEwen, I. J. *Polymer* **1983**, *24*, 1439.
(29) Cowie, J. M. G.; Ferguson, R. *J. Polym. Sci., Polym. Phys.* **1985**, *23*, 2181.
(30) Arrighi. V.; Triolo. A.; McEwen. I. J.; Holmes. P. F.; Triolo, R.; Amenitsch, H. *Macromolecules* **2000**, *33*, 4989.
(31) Holmes, P. F.; Arrighi. V.; McEwen, I. J.; Telling, M. T. F. *Nucl. Instrum. Methods B* **2003**, *200*, 411.
(32) Miller, R. L.; Boyer, R. F.; Heijboer, J. *J. Polym. Sci., Polym. Phys. Ed.* **1984**, *22*, 2021.
(33) Arrighi, V.; Holmes, P. F.; Gagliardi, S.; McEwen, I. J.; Telling M. T. F. *Appl. Phys. A, Mater. Sci. Proc.* **2002**, *74*, 466.
(34) Ribesgreus, A.; Diaz-Calleja, R.; Gargallo, L.; Radic, D. *Polymer* **1991**, *32*, 2755.
(35) Diaz-Calleja, R.; Saiz, E.; Riande, E.; Gargallo, L.; Radic, D. *J. Polym. Sci., Polym. Phys.* **1994**, *32*, 1069.
(36) Diaz-Calleja, R.; Sanchis, M. J.; Gargallo, L.; Radic, D. *J. Polym. Sci., Polym. Phys.* **1997**, *35*, 2749.
(37) Diaz-Calleja, RD.; Martinez-Pina , F.; Gargallo, L.; Radic, D. *Polymer* **2000**, *41*, 1963.
(38) Diaz-Calleja, R.; Garcia-Bernabe, A.; Sanchez-Martinez, E.; Sanchis, M. J.; Hormazabal, E. A.; Gargallo, L.; Radic, D. *J. Polym. Sci., Polym. Phys.* **2003**, *41*, 1059.
(39) Diaz-Calleja, R.; Gargallo, L.; Radic, D. *Macromolecules* **1995**, *28*, 6963.
(40) Allinger, N. L. *MMP2 (85), QCPE*, University of Indiana: Bloomfield, Indiana, 1985.
(41) McCrum, N. G.; Read, B. E.; Williams, G. *Inelastic and Dielectric Effects in Polymeric Solids*, 2nd ed.; Dover: New York, 1991.
(42) Dionisio, M.; Ramos, J. J. M.; Williams, G. *Polym. Int.* **1993**, *32*, 145.
(43) Beiner, M.; Huth, H.; Schroter, K. *J. Non-Cryst. Solids* **2001**, *279*, 126.
(44) Garwe, F.; Schonhals, A.; Lockwenz, H.; Beiner, M.; Schroter, K.; Donth, E. *Macromolecules* **1996**, *29*, 247.
(45) Johari, G. P.; Goldstein, M. *J. Chem. Phys.* **1970**, *53*, 2372.
(46) Beiner, M.; Kabisch, O.; Reichl, S.; Huth, H. *J. Non-Cryst. Solids* **2002**, *307−310*, 658.
(47) Zeeb, S.; Hijring, S.; Garwe, F.; Beiner, M.; Hempel, E.; Schonhals, A.; Schroter, K.; Donth, E. *Polymer* **1997**, *38*, 4011.
(48) Hempel, E.; Kahle, S.; Unger, R.; Donth, E. *Thermochim. Acta* **1999**, *329*, 97.

(49) Press, W. H.; Flanney, B. P.; Teukolsky, S. A.; Vetterling, W. T. *Numerical Recipes in C − The Art of Scientific Computing*, 2nd ed.; Cambridge University Press: Cambridge, 1992; p 682.
(50) Heijboer, J. In *Physics of Noncrystalline Solids*; Prins, J. A., Ed.; North-Holland: Amsterdam, 1965; p 231.
(51) de Azevedo, E. R.; Hu, W.-G.; Bonagamba, T. J.; Schmidt-Rohr, K. *J. Am. Chem. Soc.* **1999**, *121*, 8411.
(52) Schmidt-Rohr, K.; Kulik, A. S.; Beckham, H. W.; Ohlemacher, A.; Pawelzik, U.; Boeffel, C.; Spiess, H. W. *Macromolecules* **1994**, *27*, 4733.
(53) Shimizu, K.; Yano, O.; Wada, Y. *J. Polym. Sci., Polym. Phys.* **1975**, *13*, 1959.
(54) Beiner, M.; Schroter, K.; Hempel, E.; Reissig, S.; Donth, E. *Macromolecules* **1999**, *32*, 6278.
(55) Hempel, E.; Beiner, M.; Huth, H.; Donth, E. *Thermochim. Acta* **2002**, *391*, 219.
(56) Floudas, G.; Stepanek, P. *Macromolecules* **1998**, *31*, 6951.
(57) Floudas, G.; Placke, P.; Stepanek, P.; Brown, W.; Fytas, G.; Ngai, K. L. *Macromolecules* **1995**, *28*, 6799.
(58) Pineri, M.; Berticat, P.; Marchal, E. *J. Polym. Sci., Polym. Phys. Ed.* **1976**, *14*, 1325.
(59) Holmes, P. F. Ph.D. Thesis, Heriot-Watt University, 2003.
(60) Reference 51 estimates that only ∼50% of the ester groups in poly(methyl methacrylate) are sufficiently mobile to participate in the β-relaxation even above the T_g.
(61) Angell, C. A. *J. Non-Cryst. Solids* **1991**, *131−133*, 13.
(62) Böhmer, R.; Ngai, K. L.; Angell, C. A.; Plazek, D. J. *J. Chem. Phys.* **1993**, *99*, 4201.
(63) Godard, M.-E.; Saiter, J.-M. *J. Non-Cryst. Solids* **1998**, *235−237*, 635.
(64) Ngai, K. L. *J. Phys., Condens. Matter* **1999**, *11*, A119−A130.
(65) Genix, A.-C.; Laupretre, F. *Polym. Prepr.* **2003**, *44*, 305.

MA049553A